

1 Bioimpedance Based Biomarker for 2 the Detection of Precancerous and 3 Cancerous Lesions of the Pancreas: 4 Feasibility Animal Study

5 **Federica Dibennardo¹, Martina Guidetti^{1†}, Alexander Grycuk^{1‡}, Onur Fidaner¹,**
6 **Daniel S Gehrke¹, Donato Ceres¹, Margaret C John¹, Constantine H Bovalis¹, Erik**
7 **M Kundro¹, Karla Castellanos², Akshar Patel², Isaac Rajman³, Paul Grippo^{2*§}, Les**
8 **Bogdanowicz^{1*}¶**

*For correspondence:

les@novascanllc.com (LB);
pgrippo@uic.edu (PG)

[†]These authors contributed
equally to this work

[‡]These authors also contributed
equally to this work

Present address: [§]College of
Medicine, University of Illinois at
Chicago, 818 South Wolcott
Avenue, Chicago, IL 60612, USA;
[¶]NovaScan Inc., 965 W Chicago
Ave, Chicago, IL 60642, USA

9 ¹NovaScan Inc., Chicago, IL, USA; ²University of Illinois at Chicago, Chicago, IL, USA;
10 ³Texas International Endoscopy Center, Houston, TX, USA

11 **Abstract** Pancreatic cancer (PC) remains a significant healthcare challenge due to its aggressive
12 nature and poor prognosis. The current gold standard of biopsies has limited diagnostic efficacy
13 due to various shortcomings. We propose a feasibility study for the use of a bioimpedance
14 biomarker to detect PC. The biomarker was evaluated in a double blind study on ex vivo
15 pancreases of mice: 15 K-ras;Trp53;Pdx-1-Cre, 2 K-ras;Pdx-1-Cre, and 9 wild type controls (Study
16 1); to determine if the biomarker can distinguish between PC and acute pancreatitis (AP), we
17 challenged it with 18 cerulein-induced AP and 6 saline-injected controls (Study 2). The results
18 from Study 1 showed 100% specificity and 94% sensitivity against histopathology outcomes; for
19 Study 2 all AP and saline-injected pancreases were diagnosed as non-cancerous. Regression
20 analysis revealed a positive correlation between biomarker and pathologically analyzed cancer
21 induced fibrosis ($r(15)= 0.82$ ($p <0.001$)). These findings demonstrate the potential of this
22 bioimpedance biomarker as a diagnostic tool for PC.
23

25 **Introduction**

26 Pancreatic cancer (PC) accounts for half a million new cases and 4.7% of the world's cancer-related
27 deaths in 2020 *Globocan (2020)*. It is considered one of the most lethal malignancies and a sig-
28 nificant healthcare challenge *Koul et al. (2018)*. PC has the lowest survival rate among all known
29 cancers according to the American Cancer Society, due to its aggressive nature and poor prognosis
30 *CancerStatisticsCenter (2022)*; *Kato and Honda (2020)*; *Young et al. (2020)*. This is attributed to the
31 difficulty in early diagnosis and to the lack of standardized guidelines in assessing suspicious pan-
32 creatic masses *Garg and Chari (2020)*; *Yang et al. (2021)*. The complex pathophysiology, together
33 with the lack of early diagnostic and prognostic markers are major barriers at the basis of the late
34 and often incurable stage diagnosis of PC. At present, there is no standard screening procedure
35 for early detection of PC as the currently available imaging and endoscopic modalities fail to accu-
36 rately detect lesions under 3 cm *Kitano et al. (2019)* and discern malignant from benign lesions.
37 There is demand for an on-site, real-time assessment device that works as a quantitative decision
38 support tool for the endoscopist. A more timely and accurate diagnosis of PC would reduce revisits,
39 expedite treatment, and improve the current prognosis of this disease.

40 To date, PC diagnosis relies on imaging modalities, including multidetector computed tomography (MDCT), magnetic resonance imaging (MRI), and endoscopic ultrasound (EUS) *Moradi and*
41 *Iagaru (2020); Kato and Honda (2020); Michl et al. (2021); Zhang et al. (2018)*. The first modality of
42 choice for diagnosing PC is MDCT (Multidetector CT) *Zhang et al. (2018)*. While generally safe and
43 non-invasive, contrast MDCT is accompanied by the risk of nephrotoxicity from the iodine-contrast
44 agent as well as radiation exposure *Zhang et al. (2018)*. MRI is often used as a subsequent test when
45 there is a high suspicion of PC despite a clear CT *Zhang et al. (2018)*. However, both CT and MRI
46 are not very sensitive in detecting the tumor in its initial development while still small *Kitano et al.*
47 *(2019)* (typically less than 3 cm) and localized *Koul et al. (2018)*. Endoscopic ultrasound (EUS) guided
48 tissue acquisition is currently the gold standard for sampling pancreatic masses. Confirmation of
49 suspicious lesions is generally obtained via EUS guided needle biopsies, using fine-needle aspira-
50 tion (FNA) or fine needle biopsy (FNB) *bio (????); Chang et al. (1997); Varadarajulu and Wallace*
51 *(2004); Michl et al. (2021); Zhang et al. (2018)*. EUS positions an echoendoscope transducer close to
52 the pancreas, allowing for high-resolution visualization of the pancreas and the surrounding struc-
53 tures during the procedure, which increases the chances of obtaining a representative sample of
54 the tumor. Hence, it is ideal for lesions smaller than 2 cm and is relatively safe *Zhang et al. (2018);*
55 *Bispo et al. (2021); Shrikhande et al. (2012); Wang et al. (2013); Koul et al. (2018)*. Improvements in
56 fine needle biopsy (FNB) technologies and increased availability is further improving the diagnostic
57 yield of EUS guided biopsies.

58 With all these discussed modalities, confirmation of cancerous lesions is only accomplished
59 when biopsy samples are obtained and screened in an ex vivo setting by a cytopathologist. The chal-
60 lenges to successful biopsies arise from difficulties in physically locating the lesions, inter-observer
61 variability in identifying and grading the lesions, and low diagnostic yield due to insufficient integrity
62 or size of the samples. Additionally, misdiagnosis of tissues may result from pancreatitis, necro-
63 sis, or diffusely infiltrating carcinoma *Chang et al. (1997); Varadarajulu and Wallace (2004); DeWitt*
64 *et al. (2004); King et al. (2022); Yamashita et al. (2020); Bhutani et al. (2004)*. In the pancreatobiliary
65 tract, indeterminate structures often present a diagnostic challenge in differentiating benign from
66 malignant tissues *Bowlus et al. (2016)*, leading to multiple procedures that cause undue stress to
67 patients and additional costs. EUS-FNA or EUS-FNB with cytologic rapid on-site evaluation (ROSE)
68 has been introduced as an efficient diagnostic modality for evaluation of solid pancreatic lesions.
69 ROSE has advantages of providing timely feedback on sample adequacy and optimizing the num-
70 ber of needle passes performed and most of all it may increase the diagnostic yield, since malignant
71 cells that are often detected during later FNA passes would otherwise be missed if tissue sampling
72 stopped prematurely *Koul et al. (2018)*. One study revealed that EUS-FNB alone had a significantly
73 lower diagnostic accuracy than EUS-FNB and ROSE (80.7% vs 93.1%, $P = .001$), thus suggesting a po-
74 tential benefit of ROSE during these procedures *de Moura et al. (2020)*. The restricted availability of
75 ROSE and consequently, the limited accuracy of EUS-FNA or EUS-FNB in the absence of ROSE might
76 have constrained widespread utilization of EUS-guided sampling globally. Finally, these modalities
77 are implemented when there is already a high suspicion of PC, by which time cancer tends towards
78 its advanced stages, limiting curative opportunities.

79 Given the limitations of the current clinical standard for PC diagnosis, multiple research groups
80 are studying advanced methods to improve the diagnostic process for PC. Some newly developed
81 technologies focus on assessing biopsy sample adequacy and cell viability on site right after the
82 samples are collected *Pritchett et al. (2022); Duke et al. (2022)*. These methods need a small
83 amount of specimens for rapid diagnosis and provide indication of the quality of the initial sampling
84 before going for pathology or information to assess if additional samples are needed to be biop-
85 sied for a successful pathology, issuing a preliminary diagnosis in a shorter time than traditional
86 approaches *Pritchett et al. (2022); Duke et al. (2022)*. These technologies are based on different
87 principles. Ambient mass spectroscopy enables controlled delivery of a discrete water droplet to
88 a tissue surface for efficient extraction of biomolecules, which is then delivered for analysis *Zhang*
89 *et al. (2017); Lu et al. (2020)*; optical imaging techniques able to generate images reminiscent of his-

91 tology without any tissue processing *Thouvenin et al. (2021)*. Finally, there is an automatic method
92 of sample preparation to enhance the evaluation and detection of cancer *Pritchett et al. (2022)*;
93 *Duke et al. (2022)*. Though these techniques are real-time and offer a rapid and nondestructive
94 diagnosis of cancer tissues, they are characterized by some limitations, such as high cost, low reso-
95 lution *Sans et al. (2019)*; *Jain et al. (2015)*, and the potential of modifying the sample before pathol-
96 ogy assessment. Therefore, there is a need for a real-time tool that can evaluate cancer presence
97 in biopsies without affecting the sample, and requires fewer cytology and histology specimens
98 prepared and submitted, decreasing the administrative costs.

99 In this paper, the authors propose a feasibility study for the use of a novel bioimpedance based
100 biomarker - the Cole Relaxation Frequency (CRF) - to detect PC. We have previously shown The CRF
101 to quantitatively detect cancer in breast, skin, and lung tissues *Gregory et al. (2012)*; *Svoboda et al.*
102 (2018); *Bogdanowicz et al. (2022)*; *Guidetti et al. (2022)*. The aim of this pilot study is to determine
103 if the CRF based biomarker can detect PC and also discern pancreatitis from PC in the genetically
104 modified KPC and KC mouse model, acute pancreatitis mouse model and wild type controls. These
105 animal models spontaneously and progressively develop PC allowing us to correlate the biomarker
106 values with the lesions as they develop from precancerous to malignancy. The KPC mouse is an
107 established and clinically relevant model of PC which develops many key features observed in hu-
108 man PC *Hu et al. (2019)*; *Renz et al. (2018)*; *Niknafs et al. (2019)*; this work may lay the foundation
109 towards understanding the potential for CRF to inform on cancer stages in humans. Specifically,
110 the biomarker was evaluated in a double blind study on ex vivo pancreases of mice. Two studies
111 were run to determine if the biomarker could discern between K-ras;Trp53;Pdx-1-Cre, 2 K-ras;Pdx-
112 1-Cre, and 9 wild type controls and between acute pancreatitis (AP) and PC by adding to the anal-
113 ysis cerulein-induced AP and saline-injected mice. The device conducted a spectral bioimpedance
114 measurement for CRF biomarker computation. CRF based cancer determinations were compared
115 against histopathology outcomes to calculate specificity and sensitivity. These findings demon-
116 strate the potential of this bioimpedance biomarker as a diagnostic tool for PC. A future imple-
117 mentation of this technology into a digital version of ROSE device would allow the widespread use
118 of ROSE after EUS-FNAs and EUS-FNBs at accessible costs.

119 Results

120 In this study, we evaluated the bioimpedance based biomarker to detect PC in genetically modified
121 KPC and KC mouse models, acute pancreatitis mouse model and wild type controls. The KPC mouse
122 model is one of the most used models to evaluate pancreatic ductal adenocarcinoma (PDAC) due
123 to its faithful recapitulation of human pancreatic cancer biology *Hu et al. (2019)*; *Renz et al. (2018)*;
124 *Niknafs et al. (2019)*. Indeed, KPC PDACs provide a unique opportunity to analyze the evolution of
125 cancer in a controlled setting, not otherwise possible in human patients. The study involved two
126 double-blind studies on ex vivo pancreas of mice. In Study 1, the biomarker was tested in n=26
127 mice (15 KPC, 2KC, and 9 controls), in Study 2 we determined the biomarker ability to differentiate
128 PC from acute pancreatitis (AP), considering n=24 (18 cerulein-induced AP and 6 saline-injected
129 controls) (Figure 1).

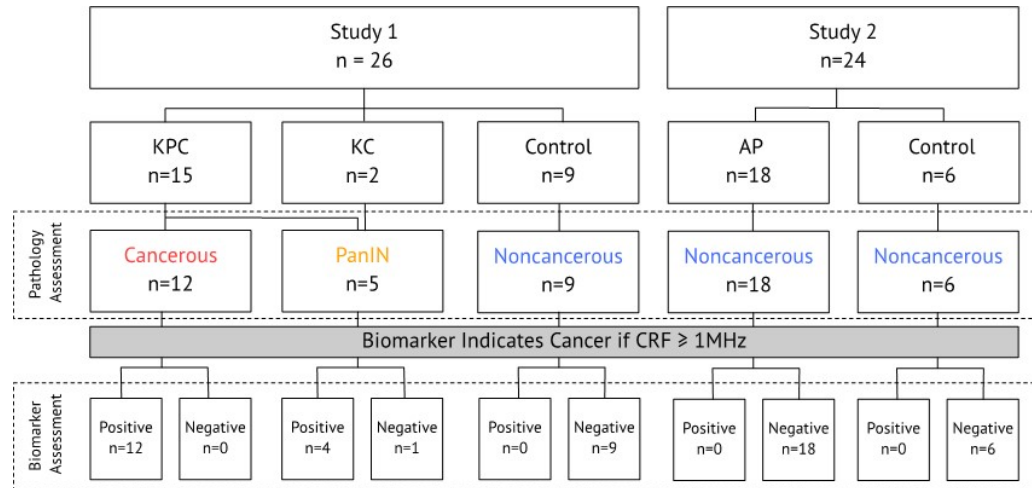


Figure 1. Study design.

130 The CRF measurements were collected at different locations on the pancreatic sample and CRF
 131 determinations allowed to calculate sensitivity and specificity against histopathology outcomes.
 132 As far as Study 1 is concerned, based on histopathology, 12 KPC pancreases were confirmed as
 133 cancerous, 9 controls were confirmed as noncancerous, while 5 pancreases (3 KPC and 2 KC) pre-
 134 sented with pancreatic intraepithelial neoplasia (PanIN), a precancerous condition. Examples of
 135 CRF curves for noncancerous, precancerous, and cancerous samples are provided in Figure 2.

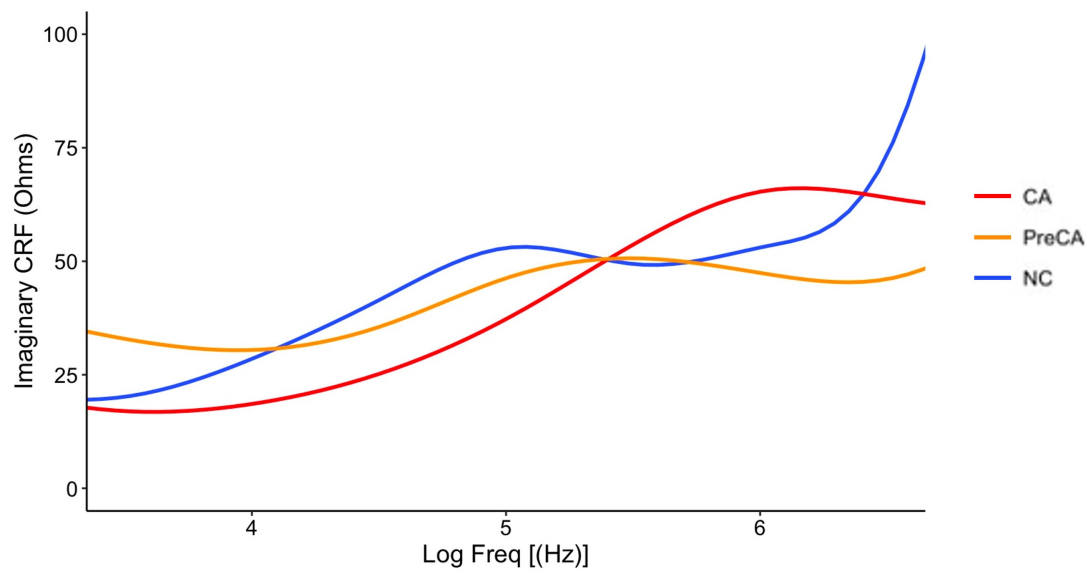


Figure 2. Example CRF curves from noncancerous (NC), precancerous (PreCA), and cancerous (CA) mice pancreases.

136 The CRF biomarker identified 4 out of 5 PanIN samples as cancerous. Considering the entire
 137 cohort for Study 1 (n=26), specificity and sensitivity were 100% and 94%, respectively. The sam-
 138 ple determinations based on the CRF biomarker are reported in Table 1. If PanIN samples were
 139 excluded, specificity and sensitivity were both 100% (n=21). The Spearman correlation coefficient
 140 between percent fibrosis and CRF was $r(15)= 0.82$ ($p < 0.001$), which indicates a strong positive cor-
 141 relation (Figure 3).

		Histology Assessment		
		CA	PreCA	NC
Biomarker Assessment	CA	12	1	0
	PreCA	1	4	0
	NC	0	0	9

Table 1. Confusion matrix for Study 1. NC: noncancerous; CA: cancerous; PreCA: precancerous.

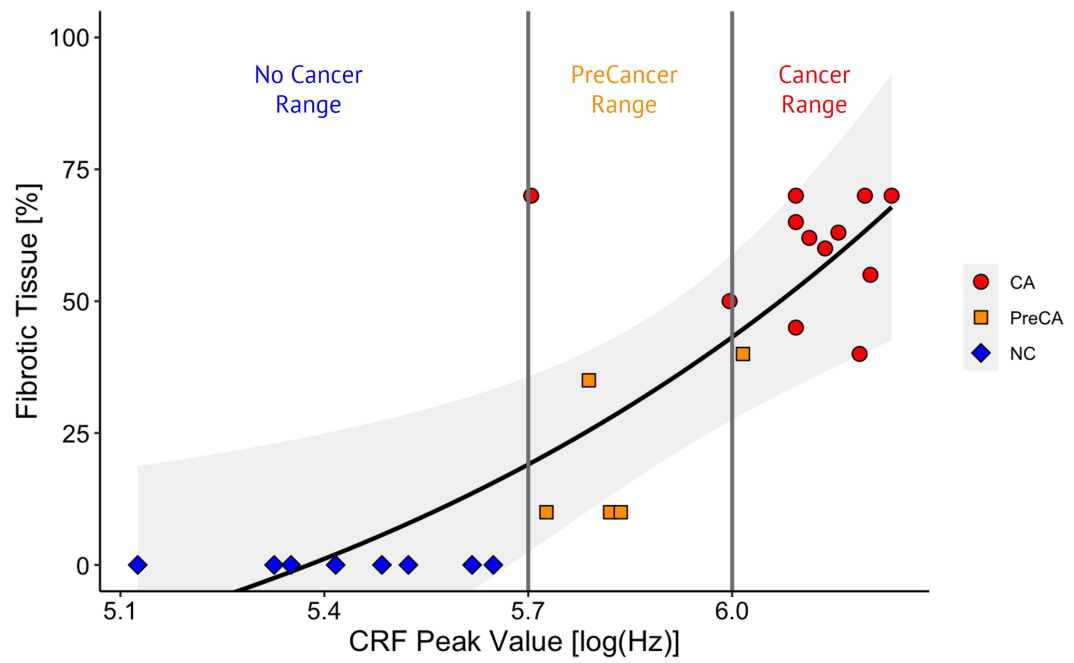


Figure 3. Spearman correlation between percent fibrosis and CRF for noncancerous, cancerous, and precancerous pancreases. Grey band shows the 99.99% confidence interval.

142 Discussion

143 This study found specificity and sensitivity of 100% and 94%, respectively, of the bioimpedance
144 based biomarker in discerning between cancerous and noncancerous pancreas tissues from mice.
145 Moreover, all pancreatitis samples were detected as noncancerous. The findings also determined
146 a strong positive correlation between CRF biomarker and percent fibrosis in cancerous and precan-
147 cerous samples. This feasibility study demonstrates the potential for the use of the CRF to predict
148 PC and the level of fibrosis in PC. The identification of malignant precursors for PanIN samples in-
149 dicates the biomarker capability to detect early-stage PCs. The biomarker was found to be strong
150 against the confounding factor of pancreatitis, demonstrating that the CRF can decipher PC from
151 normal and acute pancreatitis tissues making it an ideal clinical detection tool.

152 The positive correlation between CRF biomarker and pathologically analyzed cancer induced
153 fibrosis in PC may be similar to that shown in breast cancer *Gregory et al. (2020)*. Gregory et. al
154 *Gregory et al. (2020)* previously reported using the CRF biomarker as a prognostic indicator for
155 the aggressiveness of breast cancer. In that retrospective study, a strong correlation was found
156 between the CRF values of tumor excisions measured at time of surgery and long term patient
157 outcomes in terms of recurrence or time-cancer-free *Gregory et al. (2020)*. According to their find-
158 ing, when the CRF is below 5.3 log(Hz) it is likely that the cancer is nonrecurrent; when the CRF is
159 in the range between 5.3 log(Hz) and 5.8 log(Hz) there is a high likelihood that cancer is recurrent
160 not metastasizing; and when the CRF is above 5.8 log(Hz) then there is an increasingly greater like-
161 lihood that the cancer is recurrent with metastasis (see Figure 4) *Gregory et al. (2020)*. A similar
162 behavior was observed for the pancreatic tissues data presented in this current study (see Figure
163 3). These findings suggest that the CRF may well be a universal property of cells as they transform
164 regardless of organ origin and that the CRF biomarker may be studied as a prognostic indicator.

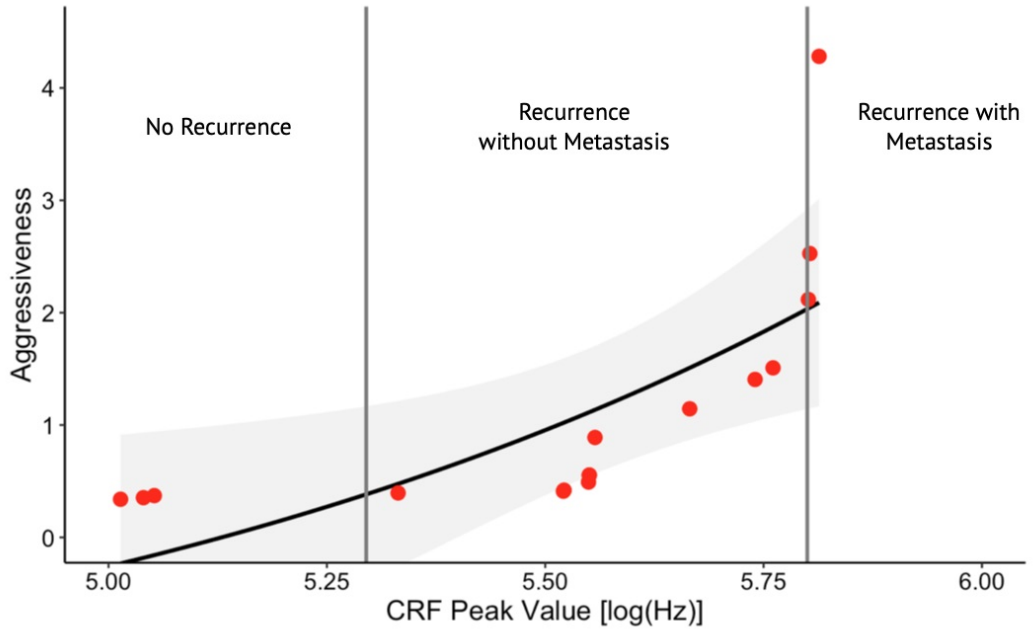


Figure 4. Gregory et al. *Gregory et al. (2020)* have showed that the CRF biomarker can retrospectively classify breast cancer data in 3 well-differentiated categories: nonrecurrent (NR); recurrent with no metastasis (RNM); and recurrent with metastasis (RM).

165 Once proven to be effective in a larger preclinical and clinical trial, the CRF based technology
 166 could be implemented into a medical device for clinical use. Indeed, the electrodes used to mea-
 167 sure the bioimpedance could be developed into a rapid onsite evaluation device that would be
 168 used as an ex vivo decision support tool for real-time quantitative assessment of biopsy samples.
 169 Another future development can be seen in the implementation of the measuring electrodes on
 170 the tip of an endoscopic device for in vivo clinical use to assist endoscopists in the decision-making
 171 process and to guide them in margin assessment and biopsies acquisition.

172 This study is not without limitations. We expect some level of variability when transferring
 173 these results to a clinical trial. A larger sample size could allow for a deeper understanding of
 174 the potential use of the biomarker for early detection of PC. This study did not include chronic
 175 pancreatitis samples, however a standard model for this disease is already available and will be
 176 included in a future study by the group.

177 Methods and Materials

178 Background

179 Several studies *Qiao et al. (2010); Han et al. (2007); Gregory et al. (2012); Svoboda et al. (2018);*
 180 *Shell and Gregory (2017); Gabriel et al. (1996)* have demonstrated that different tissue types and
 181 cells behaviors, including cancer, can be identified by measuring frequency dependent bioelectri-
 182 cal properties. The cell membrane behaves like an electrical capacitor in that a charge (ion) brought
 183 up to the outside of the membrane causes charges of the opposite sign to deploy on the interior
 184 face of the membrane. This process then stores equal amounts of electrical charge of opposite
 185 sign on each side of the membrane. However, this charge can be neutralized by charges flow-
 186 ing in the opposite direction through resistive paths between the inside and outside of the cell
 187 membrane. Some possible paths are via proteins embedded in the membrane; further paths are
 188 possible by a split of the current passing through the cell or around the cell. The behavior of the

189 cell membrane has been described with the circuit diagram (Cole-Cole model). Current passing
 190 through the extracellular matrix encounters only resistive impedance to the current flow, as does
 191 the current passing through the proteins in the membrane wall with current passing around the
 192 cell. A portion of the current also passes through the capacitive membrane, and this has a complex
 193 behavior that can be mathematically modeled. The characteristic rate at which a cell redistributes
 194 electrical charge on and off the cell membrane, so that the charge gets equilibrated, is called Cole
 195 Relaxation Frequency (CRF). By examining the transmembrane cellular response in the frequency
 196 range of 1 KHz to 10 MHz, also known as the β region, cancerous tissues can be detected. To char-
 197 acterize spectral bioimpedance measurements, Novascan has developed an algorithm that utilizes
 198 the equivalent circuit proposed by Cole et al. *Cole and Cole (1941)*. The circuit is described by the
 199 following equation: $Z = Z' + jZ'' = R_\infty + \frac{R_0 - R_\infty}{1 + (j \frac{f}{CRF})^\alpha}$, where Z is the complex sample impedance,
 Z' is the real, and Z'' is the imaginary component of Z , R_0 and R_∞ respectively represent the low and
 201 high frequency limits of Z , f is the measurement frequency, CRF is the Cole Relaxation Frequency, j
 202 is the imaginary unit and α is a dimensionless number that is inversely related to the broadening in
 203 the frequency domain of Z' , and the spread of the peak seen in $-Z''$. The algorithm extracts the CRF
 204 that is used as an impedance spectroscopy biomarker to detect cancer. NovaScan has established
 205 proof-of-concept technologies to detect cancer in breast *Gregory et al. (2012, 2020)*, skin *Svoboda*
 206 *et al. (2018)*, and lung *Bogdanowicz et al. (2022); Guidetti et al. (2022)* tissues. Moreover, for each
 207 tissue kind, NovaScan has developed customized prototype devices that have been tested and val-
 208 idated *ex vivo* *Gregory et al. (2012); Svoboda et al. (2018); Bogdanowicz et al. (2022); Guidetti et al.*
 209 *(2022)*. We based the feasibility of the current work on these previous studies and on the work by
 210 Subramanian et al., which illustrated cell architecture derangement across tumor formation, fur-
 211 ther explaining the physical foundation of CRF deviations observed for cancer *Subramanian et al.*
 212 *(2009)*.

213 **Mouse Model**

214 The KPC (Pdx1-Cre/LSL-Kras^{G12D}/LSL-p53^{R172H}) murine model is the most employed *in vivo* preclin-
 215 ical tool for studying PC. Mutations in both endogenous KrasG12D (K) and p53R172H (P) alleles
 216 accompanied by the Lox-STOP-Lox (LSL) insert are simultaneously expressed following Cre (C) in-
 217 duction regulated by the Pdx1 promoter. The phenotypic result triggers the initiation of a high
 218 frequency of Pancreatic Intraepithelial Neoplasia (PanIN) lesions that can progress to pancreatic
 219 ductal adenocarcinoma (PDAC) *Hu et al. (2019)*. In order to avoid variance in observations from
 220 chimeric strains, KPC mice in the B6 strain background develop PanINs at 4-5 weeks, local invasive
 221 cancer at 10-12 weeks and more advanced disease at 16-22 weeks, with metastasis in 40% of spec-
 222 imens. The KPC mouse model is among the most commonly used models for studying PDAC due
 223 to its faithful recapitulation of human pancreatic cancer biology *Hu et al. (2019); Renz et al. (2018);*
 224 *Niknafs et al. (2019); Gabriel et al. (2020); Vernucci et al. (2019)*. A timely study of the prognostic
 225 value of CRF would be challenging with human tissue *ex vivo* (5-10 yr study) and almost impossible
 226 *in vivo*. KPC PDACs provide a unique opportunity to study the evolution of cancer in a controlled
 227 setting, not otherwise possible in human patients.

228 **Study Design and Methods**

229 We evaluated the biomarker in a double blind study on *ex vivo* pancreases of mice. An initial study
 230 included 15 K-ras;Trp53;Pdx-1-Cre, 2 K-ras;Pdx-1-Cre, and 9 wild type controls; to determine if the
 231 biomarker could distinguish between PC and acute pancreatitis (AP), in a secondary study we chal-
 232 lenged it with 18 cerulein-induced AP (3 groups at 24, 48, 72 hours, n=6 for each group) and 6
 233 saline-injected controls. All tests were performed in multiple locations of the pancreases using a
 234 custom-built bioelectrical impedance measurement device and tetrapolar electrodes. The tetrap-
 235 polar configuration is comprised of 4 electrodes including a source electrode (for the generation
 236 of the stimulating high-frequency signal), a drain electrode (for the measurement of the current

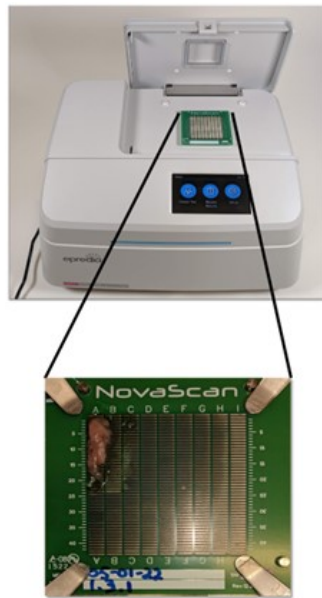


Figure 5. Bioimpedance spectroscopy scanning device with measurement electrode array used for a series of spectral bioimpedance measurements. A zoom in of the electrode with a pancreas sample is also shown.

237 through a precision 50 Ohm shunt resistor), and two pick up electrodes placed between the source
 238 and the drain (for the measurement of the voltage drop across the tissue). The device performed a
 239 bioelectrical impedance measurement of the samples over a frequency range of 1 KHz to 20 MHz.
 240 The measurements of the biological sample were done using an analog heterodyne-type circuit
 241 in which the measured high frequency signals from each electrode were demodulated to a low-
 242 frequency signal that was then sampled by analog-to-digital converters (ADC). This information
 243 was processed further by a micro-controller to extract the magnitude and phase of the measured
 244 voltages as complex numbers. The impedance was then computed as the complex ratio between
 245 the voltage drop across the pick-up electrodes and current passed through the drain electrode.
 246 The impedance values were then sent to a PC where they were displayed in their Real and Imaginary
 247 components for further analysis and determination of the Cole Relaxation Frequencies (CRF).
 248 An array of electrodes was used to map the tissue samples. The electrode array was manufactured
 249 on a standard PCB featuring 400 1x4mm copper pads spaced by 0.5 mm, finished by immersion
 250 silver and chlorination to function as Ag/AgCl electrodes. The electrodes are electrically connected
 251 to contact pads on the back side of the PCB through vias. An XYZ motorized stage was used to
 252 move four pogo pins to make contacts to back-side contact pads. Each pogo pin is connected to
 253 the custom-made electronics for impedance measurement as described above. A custom GUI al-
 254 lowed for the synchronously motion the XYZ and recording the impedance at each location of the
 255 sample in order to build an impedance map.

256 Cancer determination was made when the CRF parameter was measured above 1 MHz (Figure
 257 1). All samples were processed by standard histopathology after bioimpedance testing. Sensitivity
 258 and specificity of CRF based outcomes were determined against histopathology outcomes as
 259 ground truth. During histopathology pancreases were also assessed for percent fibrosis averaging
 260 over multiple fields of view. Spearman's correlation was used to determine if there was any corre-
 261 lation between percent fibrosis and CRF. An a priori α -value was set at 0.01 to indicate statistical
 262 significance. All statistical analyses were performed in R.

263 Acknowledgments

264 Additional information can be given in the template, such as to not include funder information in
 265 the acknowledgments section.

266 References

267 Biopsy – Pancreatic Cancer Action Network.; <https://www.pancan.org/facing-pancreatic-cancer/diagnosis/biopsy/#challenges>.

268

269 **Bhutani M**, Gress F, Giovannini M, Erickson R, Catalano M, Chak A, Deprez PH, Faigel D, Nguyen C. The No Endosonographic Detection of Tumor (NEST) Study: a case series of pancreatic cancers missed on endoscopic ultrasonography. *Endoscopy*. 2004; 36(05):385–389.

270

271

272 **Bispo M**, Marques S, Rio-Tinto R, Fidalgo P, Devière J. The role of endoscopic ultrasound in pancreatic cancer staging in the Era of neoadjuvant therapy and personalised medicine. *GE-Portuguese Journal of Gastroenterology*. 2021; 28(2):111–120.

273

274

275 **Bogdanowicz L**, Fidaner O, Ceres D, Grycuk A, Guidetti M, Demos D, et al. The Cole Relaxation Frequency as a Parameter to Identify Cancer in Lung Tissue: Preliminary Animal and Ex Vivo Patient Studies. *JMIR Biomedical Engineering*. 2022; 7(1):e35346.

276

277

278 **Bowlus CL**, Olson KA, Gershwin ME. Evaluation of indeterminate biliary strictures. *Nature Reviews Gastroenterology & Hepatology*. 2016; 13(1):28–37.

279

280 **CancerStatisticsCenter**, Analysis Tool | American Cancer Society - Cancer Facts Statistics. 5-year relative survival, 2011–2017.; 2022. <https://cancerstatisticscenter.cancer.org/#!/data-analysis/SurvivalByStage>.

281

282 **Chang KJ**, Nguyen P, Erickson RA, Durbin TE, Katz KD. The clinical utility of endoscopic ultrasound-guided fine-needle aspiration in the diagnosis and staging of pancreatic carcinoma. *Gastrointestinal endoscopy*. 1997; 45(5):387–393.

283

284

285 **Cole KS**, Cole RH. Dispersion and absorption in dielectrics I. Alternating current characteristics. *The Journal of chemical physics*. 1941; 9(4):341–351.

286

287 **DeWitt J**, Devereaux B, Chriswell M, McGreevy K, Howard T, Imperiale TF, Ciaccia D, Lane KA, Maglinte D, Kopecky K, et al. Comparison of endoscopic ultrasonography and multidetector computed tomography for detecting and staging pancreatic cancer. *Annals of internal medicine*. 2004; 141(10):753–763.

288

289

290 **Duke JD**, Sturgis CD, Hartley C, Bailey M, Reid M, Kern R, Bluestone A, Subramanian H, Reisenauer J. Evaluation of Automated Sample Preparation System for Lymph Node Sampling. . 2022; .

291

292 **Gabriel ANA**, Jiao Q, Yvette U, Yang X, Al-Ameri SA, Du L, Wang Ys, Wang C. Differences between KC and KPC pancreatic ductal adenocarcinoma mice models, in terms of their modeling biology and their clinical relevance. *Pancreatology*. 2020; 20(1):79–88.

293

294

295 **Gabriel S**, Lau R, Gabriel C. The dielectric properties of biological tissues: III. Parametric models for the dielectric spectrum of tissues. *Physics in medicine & biology*. 1996; 41(11):2271.

296

297 **Garg SK**, Chari ST. Early detection of pancreatic cancer. *Current opinion in gastroenterology*. 2020; 36(5):456–461.

298

299 **Globocan PS**, Pancreas Statistics Globocan 2020 | WHO.; 2020. <https://gco.iarc.fr/today/data/factsheets/cancers/13-Pancreas-fact-sheet.pdf>.

300

301 **Gregory W**, Marx J, Gregory C, Mikkelsen W, Tjoe J, Shell J. The Cole relaxation frequency as a parameter to identify cancer in breast tissue. *Medical physics*. 2012; 39(7Part1):4167–4174.

302

303 **Gregory WD**, Christie SM, Shell J, Nahhas GJ, Singh M, Mikkelsen W. Cole relaxation frequency as a prognostic parameter for breast cancer. *Journal of Patient-Centered Research and Reviews*. 2020; 7(4):343.

304

305 **Guidetti M**, BOGDANOWICZ L, FIDANER O, CERES D, GRYCUK A, GEHRKE DS, HOELLER M, BOVALIS C, DEMOS D. COLE RELAXATION FREQUENCY: A PARAMETER TO ASSESS LYMPH NODE STATUS IN PATIENTS WITH LUNG CANCER. *Chest*. 2022; 162(4):A1659–A1660.

306

307

308 **Han A**, Yang L, Frazier AB. Quantification of the heterogeneity in breast cancer cell lines using whole-cell impedance spectroscopy. *Clinical cancer research*. 2007; 13(1):139–143.

309

310 **Hu S**, Pan L, Shangguan J, Figini M, Eresen A, Sun C, Wang B, Ma Q, Hu C, Yaghmai V, et al. Non-invasive dynamic monitoring initiation and growth of pancreatic tumor in the LSL-KrasG12D/+; LSL-Trp53R172H/+; Pdx-1-Cre (KPC) transgenic mouse model. *Journal of immunological methods*. 2019; 465:1–6.

311

312

313 **Jain M**, Robinson BD, Salamoon B, Thouvenin O, Boccara C, Mukherjee S. Rapid evaluation of fresh ex vivo
314 kidney tissue with full-field optical coherence tomography. *Journal of pathology informatics*. 2015; 6(1):53.

315 **Kato S**, Honda K. Use of biomarkers and imaging for early detection of pancreatic cancer. *Cancers*. 2020;
316 12(7):1965.

317 **King D**, Kamran U, Dosanjh A, Coupland B, Mytton J, Leeds JS, Nayar M, Patel P, Oppong KW, Trudgill NJ. Rate
318 of pancreatic cancer following a negative endoscopic ultrasound and associated factors. *Endoscopy*. 2022; .

319 **Kitano M**, Yoshida T, Itonaga M, Tamura T, Hatamaru K, Yamashita Y. Impact of endoscopic ultrasonography
320 on diagnosis of pancreatic cancer. *Journal of gastroenterology*. 2019; 54(1):19–32.

321 **Koul A**, Baxi AC, Shang R, Meng X, Li L, Keilin SA, Willingham FF, Cai Q. The efficacy of rapid on-site evaluation
322 during endoscopic ultrasound-guided fine needle aspiration of pancreatic masses. *Gastroenterology Report*.
323 2018; 6(1):45–48.

324 **Lu H**, Zhang H, Wei Y, Chen H. Ambient mass spectrometry for the molecular diagnosis of lung cancer. *Analyst*.
325 2020; 145(2):313–320.

326 **Michl P**, Löhr M, Neoptolemos JP, Capurso G, Rebours V, Malats N, Ollivier M, Ricciardiello L. UEG position
327 paper on pancreatic cancer. Bringing pancreatic cancer to the 21st century: Prevent, detect, and treat the
328 disease earlier and better. *UEG journal*. 2021; 9(7):860–871.

329 **Moradi F**, Iagaru A. The role of positron emission tomography in pancreatic cancer and gallbladder cancer. In: *Seminars in Nuclear Medicine*, vol. 50 Elsevier; 2020. p. 434–446.

330 **de Moura DT**, McCarty TR, Jirapinyo P, Ribeiro IB, Hathorn KE, Madruga-Neto AC, Lee LS, Thompson CC. Evaluation
331 of endoscopic ultrasound fine-needle aspiration versus fine-needle biopsy and impact of rapid on-site
332 evaluation for pancreatic masses. *Endoscopy International Open*. 2020; 8(06):E738–E747.

333 **Niknafs N**, Zhong Y, Moral JA, Zhang L, Shao MX, Lo A, Makohon-Moore A, Iacobuzio-Donahue CA, Karchin R.
334 Characterization of genetic subclonal evolution in pancreatic cancer mouse models. *Nature communications*.
335 2019; 10(1):1–10.

336 **Pritchett MA**, D DUKE J, WILLIAMS J, SCHIRMER C, D STURGIS C, HARTLEY C, BARI M, BLUESTONE AL, SUBRAMANIAN H, MAHAJAN AK, et al. AUTOMATED SAMPLE PREPARATION SYSTEM FOR ENDOBRONCHIAL ULTRASOUND (EBUS): ROSE APPLICATIONS. *Chest*. 2022; 162(4):A1863–A1864.

337 **Qiao G**, Duan W, Chatwin C, Sinclair A, Wang W. Electrical properties of breast cancer cells from impedance
338 measurement of cell suspensions. In: *Journal of Physics: conference series*, vol. 224 IOP Publishing; 2010. p.
339 012081.

340 **Renz BW**, Takahashi R, Tanaka T, Macchini M, Hayakawa Y, Dantes Z, Maurer HC, Chen X, Jiang Z, Westphalen
341 CB, et al. β 2 adrenergic-neurotrophin feedforward loop promotes pancreatic cancer. *Cancer cell*. 2018;
342 33(1):75–90.

343 **Sans M**, Zhang J, Lin JQ, Feider CL, Giese N, Breen MT, Sebastian K, Liu J, Sood AK, Eberlin LS. Performance of
344 the MasSpec Pen for rapid diagnosis of ovarian cancer. *Clinical chemistry*. 2019; 65(5):674–683.

345 **Shell J**, Gregory WD. Efficient cancer detection using multiple neural networks. *IEEE journal of translational
346 engineering in health and medicine*. 2017; 5:1–7.

347 **Shrikhande SV**, Barreto SG, Goel M, Arya S. Multimodality imaging of pancreatic ductal adenocarcinoma: a
348 review of the literature. *HPB*. 2012; 14(10):658–668.

349 **Subramanian H**, Roy HK, Pradhan P, Goldberg MJ, Muldoon J, Brand RE, Sturgis C, Hensing T, Ray D, Bogojevic
350 A, et al. Nanoscale cellular changes in field carcinogenesis detected by partial wave spectroscopy. *Cancer
351 research*. 2009; 69(13):5357–5363.

352 **Svoboda RM**, Gharia MJ, Shell J, Gregory WD. Bioimpedance measurement as an assessment of margin pos-
353 itivity in Mohs surgical specimens of nonmelanoma skin cancer: Management implications. *Journal of the
354 American Academy of Dermatology*. 2018; 79(3):591–593.

355 **Thouvenin O**, Scholler J, Mandache D, Mathieu MC, Lakhdar AB, Darche M, Monfort T, Boccara C, Olivo-Marin
356 JC, Grieve K, et al. Automatic diagnosis and biopsy classification with dynamic full-field OCT and machine
357 learning. . 2021; .

358

361 **Varadarajulu S**, Wallace MB. Applications of endoscopic ultrasonography in pancreatic cancer. *Cancer Control*.
362 2004; 11(1):15–22.

363 **Vernucci E**, Abrego J, Gunda V, Shukla SK, Dasgupta A, Rai V, Chaika N, Buettner K, Illies A, Yu F, et al. Metabolic
364 alterations in pancreatic cancer progression. *Cancers*. 2019; 12(1):2.

365 **Wang W**, Shpaner A, Krishna SG, Ross WA, Bhutani MS, Tamm EP, Raju GS, Xiao L, Wolff RA, Fleming JB, et al. Use
366 of EUS-FNA in diagnosing pancreatic neoplasm without a definitive mass on CT. *Gastrointestinal endoscopy*.
367 2013; 78(1):73–80.

368 **Yamashita Y**, Kitano M, Ashida R. Value of endoscopy for early diagnosis of pancreatic carcinoma. *Digestive
369 Endoscopy*. 2020; 32(1):27–36.

370 **Yang J**, Xu R, Wang C, Qiu J, Ren B, You L. Early screening and diagnosis strategies of pancreatic cancer: a
371 comprehensive review. *Cancer Communications*. 2021; 41(12):1257–1274.

372 **Young MR**, Abrams N, Ghosh S, Rinaudo JAS, Marquez G, Srivastava S. Prediagnostic image data, artificial
373 intelligence, and pancreatic cancer: a tell-tale sign to early detection. *Pancreas*. 2020; 49(7):882–886.

374 **Zhang J**, Rector J, Lin JQ, Young JH, Sans M, Katta N, Giese N, Yu W, Nagi C, Suliburk J, et al. Nondestructive
375 tissue analysis for ex vivo and in vivo cancer diagnosis using a handheld mass spectrometry system. *Science
376 translational medicine*. 2017; 9(406):eaan3968.

377 **Zhang L**, Sanagapalli S, Stoita A. Challenges in diagnosis of pancreatic cancer. *World journal of gastroenterology*.
378 2018; 24(19):2047.